Mon. Not. R. Astron. Soc. **000**, 000–000 (0000)   Printed 5 February 2008   (MN LATEX style file v2.2)

Absence of H I in the Boötes Dwarf Spheroidal Galaxy

Jeremy Bailin[1] & Alyson Ford[1,2]
[1] *Centre for Astrophysics and Supercomputing, Swinburne University of Technology, Mail H39, PO Box 218, Hawthorn, Victoria, 3122, Australia; jbailin@astro.swin.edu.au*
[2] *Australia Telescope National Facility, CSIRO, P. O. Box 76, Epping NSW 1710, Australia*

arXiv:astro-ph/0611693v1 21 Nov 2006

Accepted 2006 November 21. Received 2006 November 14; in original form 2006 October 24

ABSTRACT

Neutral hydrogen (H I) observations towards the Boötes dwarf spheroidal (dSph) galaxy (hereafter Boötes), a very low luminosity metal-poor Galactic satellite, were obtained using the Parkes Radio Telescope. We do not detect any H I in or around Boötes to a 3σ upper limit of 180 $M_\odot$ within the optical half light radius and 8000 $M_\odot$ within 1.6 kpc. Its H I mass-to-light ratio is less than 0.002 $M_\odot/L_\odot$, making Boötes one of the most gas-poor galaxies known. Either reionisation severely inhibited gas infall onto the proto-Boötes, or large amounts of gas have been removed by ram pressure and/or tidal stripping. Since Boötes lies on the mass-metallicity fundamental line, this relation and the inefficiency of star formation at the faintest end of the galaxy luminosity function must be partly driven, or at least not disrupted, by extreme gas loss in such low luminosity galaxies. We also do not detect any H I associated with the leading tidal tail of the Sagittarius dSph galaxy, which fortuitously passes through the observed field, to a 3σ column density limit of 2×10^{17} cm^{-2}. This suggests that either the leading gaseous tail is ionised, or the gas in the trailing tail was removed before the current tidal disruption of the parent dSph began.

Key words: galaxies: individual: Boo dSph, Sgr dSph – galaxies: dwarf – Local Group – galaxies: ISM – galaxies: evolution

1 INTRODUCTION

Analysis of the stellar distribution in the Sloan Digital Sky Survey has led to the recent discovery of many very faint dwarf satellite galaxies of the Milky Way (Willman et al. 2005; Zucker et al. 2006a,b; Belokurov et al. 2006a,b; Grillmair 2006). Among the least luminous is the $M_V = -5.7$ satellite in Boötes that was discovered by Belokurov et al. (2006a) and has an estimated distance of 60 kpc, with a right ascension (RA) of $14^{\mathrm{h}}00^{\mathrm{m}}06^{\mathrm{s}}$ and declination of $+14^\circ30'00''$ ($l = 358\overset{\circ}{.}1$ and $b = 69\overset{\circ}{.}6$ in Galactic coordinates). Its central surface brightness is $\mu_{0,V} \approx 28$ mag arcsec^{-2} with an optical half-light radius of $13'$. Muñoz et al. (2006) obtained spectra of a number of red giant branch and asymptotic giant branch stars in Boötes and found a heliocentric systemic velocity of 95.6 km s^{-1} (or $v_{\mathrm{LSR}} = 106.2$ km s^{-1}, where v_{LSR} is the velocity with respect to the Local Standard of Rest) and a velocity dispersion of 6.6 km s^{-1}. This implies a dynamical mass of $\approx 10^7$ $M_\odot$, similar to that of most low luminosity dwarfs (Mateo 1998). The combined spectra of Boötes member stars are consistent with a metallicity of [Fe/H] ~ -2.5, making it the most metal-poor galaxy known in the Local Group. From the periods of 15 RR Lyrae variable stars in Boötes, Siegel (2006) also calculated a metallicity of [Fe/H] ~ -2.5 and a distance of 62 ± 4 kpc.

Based on the population of red giant branch stars in its colour magnitude diagram, Muñoz et al. (2006) suggested that the luminosity of Boötes may be a factor of almost five larger than the estimate of Belokurov et al. (2006a), implying $M_V = -7.5$. Siegel (2006) also argued for a high luminosity based on the population of RR Lyrae stars. Further support for this higher luminosity comes from the "fundamental line", a tight correlation between the mass-to-light ratio, metallicity, and central surface brightness of Local Group satellite galaxies (Prada & Burkert 2002). Assuming [Fe/H] $= -2.5$ and $\mu_{0,V} = 28$ mag arcsec^{-2}, this relation predicts a dynamical mass-to-light ratio for Boötes of $M/L_V \approx 150$ $M_\odot/L_\odot$, in agreement with the higher luminosity estimate of Muñoz et al. (2006), which we therefore adopt. The continuation of the fundamental line down to the most metal-poor galaxy in the Local Group makes Boötes an ideal place to probe the origin of the relation.

Although the environs of the Milky Way contain a number of low-mass faint dwarf galaxies, cosmological simulations predict an even larger number of potential host subhaloes (Klypin et al. 1999; Moore et al. 1999). A natural interpretation for this discrepancy is that lower-mass haloes are increasingly inefficient at converting their primordial baryons into stars. This interpretation is bolstered by the internal kinematics of the lowest luminosity dwarfs, whose luminosities drop dramatically as they approach a universal halo mass of 10^7 $M_{\odot}$, suggesting that this is the critical mass for efficient star formation (Mateo 1998).

Gas loss from supernova feedback and stellar winds have been invoked to explain both the low luminosities of low-mass galaxies and the mass-metallicity relation (Dekel & Woo 2003; Read et al. 2006). In the vicinity of larger galaxies, gas can also be lost to ram pressure stripping (Blitz & Robishaw 2000; Grebel et al. 2003), tidal stripping (Connors et al. 2006), or both (Mayer et al. 2006). In contrast, hydrodynamic simulations of dwarf galaxies by Tassis et al. (2006) and Brooks et al. (2006) suggest that the low star formation efficiency is driven not by gas loss but by self-regulated star formation consistent with the Kennicutt (1998) star formation law. Reionisation may also dramatically reduce the number of baryons available to form stars in many low-mass haloes (Kepner et al. 1997; Bullock et al. 2000; Dong et al. 2003).

The predicted properties of the interstellar media of dwarf galaxies are different in each of these scenarios. If dwarf galaxies are inefficient at converting their available baryons into stars then they will still contain large reservoirs of gas. On the other hand, tidal stripping leaves streams of gas extending both in front of and behind dwarfs, while ram pressure stripping leaves only trailing streams. If reionisation inhibits gas infall then there will be no discernible gas associated with dwarfs.

Blitz & Robishaw (2000) examined the Leiden-Dwingeloo H I Survey (Hartmann & Burton 1997, LDS; see also Kalberla et al. 2005) for H I emission associated with most Local Group dSph galaxies. They found that many dSphs contain large amounts of gas, with typical velocity widths of 20 km s^{-1}, but that those within 250 kpc of either the Milky Way or M31 are devoid of H I (see also Burton & Lockman 1999). They argued that ram pressure stripping is responsible for this deficit of gas among nearby satellites.

The relative proximity of the Boötes dSph galaxy allows us to detect very small quantities of gas and probe the relationship between stellar mass, gas mass and dynamical mass at the faintest end of the galaxy luminosity function. In this paper we present H I observations in the direction of Boötes, obtain strict upper limits for its H I mass, and use those limits to constrain the origin of its extremely low luminosity. By coincidence, the leading stellar tidal tail of the Sagittarius dSph galaxy, another satellite of the Milky Way which is in the process of tidal disruption, passes in front of Boötes along the line of sight (Muñoz et al. 2006). H I has been identified in the trailing tail (Putman et al. 2004), but none has yet been detected in the leading tail as might be expected if the gas were tidally stripped along with the stars. We obtain strict upper limits on the column density of H I associated with the Sagittarius leading tail.

2 OBSERVATIONS AND DATA REDUCTION

Observations were obtained at the 64m Parkes Radio Telescope in June 2006 using the 20cm multibeam receiver (Staveley-Smith et al. 1996). The 13 beams of the receiver are arranged in a hexagonal pattern with a $96'$-wide footprint. To ensure full spatial sampling within the inner $\sim2\overset{\circ}{.}5 \times 2\overset{\circ}{.}5$ of the field and to reduce artefacts introduced by scanning, scans in both constant RA and declination were observed, at a rate of 1° $\min^{-1}$. Each scan was $2^{\circ}9'$ in length and adjacent scans were offset by $32'$. An approximately $3^{\circ} \times 3^{\circ}$ field was mapped, with 33 sets of 3 RA scans interleaved with 32 sets of 3 declination scans, or 195 individual scans total. To provide wider spatial coverage, these data were combined with 9 declination scans 8° in length spanning an area approximately $6^{\circ} \times 8^{\circ}$ centred on Boötes.

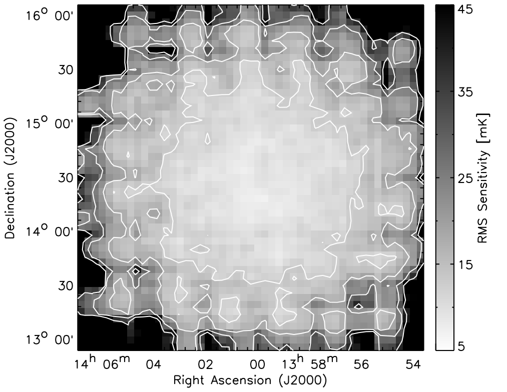

Figure 2. Map of the rms sensitivity achieved in each 0.8 km s^{-1} channel. Contours are drawn at 12.5, 17.5, 25, and 35 mK.

The receiver was operated in frequency switching mode with a throw of 3.125 MHz centred on 1420.4015 MHz, with 2048 channels over an 8 MHz bandwidth, resulting in a velocity coverage of $-400 \leq v_{\rm LSR} \leq 450$ km s^{-1} and a channel width of 0.8 km s^{-1}. The spatial resolution of the data is $15'$. Fluxes were calibrated from observations of the standards S6, S8, and S9 (Williams 1973). Although the data have not been corrected for stray radiation, it is unlikely to impact our observations due to the high Galactic latitude of the observed field.

Raw data were reduced using Livedata and then gridded into a 3D cube using Gridzilla, where data from beam 12 were omitted due to a failure of one of its low noise amplifiers. All analysis of the data cube was performed using IDL. After bandpass calibration, baseline residuals at the 10 mK level were present; we therefore corrected for these residuals by determing the baseline on a pixel-by-pixel basis using a median filter of width 50 km s^{-1}. This provided a good baseline fit except at $-60 \leq v_{\rm LSR} \leq 60$ km s^{-1}, where Galactic emission biases the median. Therefore, when analysing the data at the expected Sagittarius stream velocity (Muñoz et al. 2006), we fitted a 3rd-degree polynomial over a 50 km s^{-1} wide velocity range surrounding $v_{\rm LSR} = 60$ km s^{-1}. Examples of this process are shown in Figure 1.

The rms brightness temperature sensitivity achieved in each channel varies across the field due to the arrangement of the beams, with a maximum sensitivity of 7 mK and a median sensitivity of 13 mK within $1\overset{\circ}{.}5$ of the field centre. The sensitivity was empirically determined for each pixel from the rms dispersion in an emission-free region of the spectrum after baseline subtraction, and is shown in Figure 2.

Examination of individual channel maps reveals that

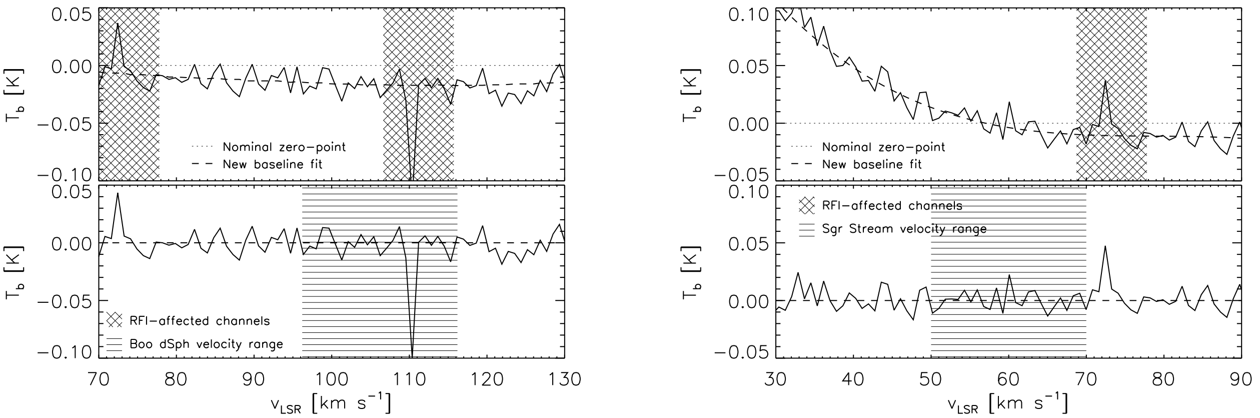

Figure 1. *(Top-left)* Spectrum at the location and velocity of Boötes after initial data reduction. The dotted line indicates the nominal zero-point while the dashed line shows our adopted baseline. The cross-hatched region indicates channels suffering from low-level RFI. *(Bottom-left)* As above but corrected for the new baseline. The shaded region shows a 20 km s^{-1} velocity range around the nominal Boötes velocity. *(Right)* As in the left panels but at the velocity expected for the Sagittarius leading tidal tail. Local Galactic emission is visible at the lower velocities.

Table 1. Boo dSph Line Fluxes

Aperture Radius	Integrated Line Flux [K km s^{-1}]	$\langle N_{\mathrm{H\,I}} \rangle$ [10^{16} cm^{-2}]	$M_{\mathrm{H\,I}}$ [M$_\odot$]
1 pixel	-0.010 ± 0.028	-1.7 ± 5.1	-7 ± 20^a
13′	-0.010 ± 0.014	-1.7 ± 2.5	-23 ± 33
30′	-0.017 ± 0.012	-3.0 ± 2.1	-220 ± 150
60′	-0.013 ± 0.012	-2.4 ± 2.2	-670 ± 620
90′	-0.012 ± 0.012	-2.3 ± 2.2	-1400 ± 1400

[a] Equivalent mass within the beam half power radius.

the data over velocity ranges of $68.7 \leq v_{\mathrm{LSR}} \leq 77.8$ km s^{-1} and $106.7 \leq v_{\mathrm{LSR}} \leq 115.7$ km s^{-1} are affected by low-level radio frequency interference (RFI) of unknown origin. We mask out all affected channels in the analysis and discuss the effects on our upper limits in § 3.

3 RESULTS FOR BOO DSPH

We find no evidence of H I emission at the velocity of Boötes. In Figure 3 we present the zeroth moment map integrated over a velocity width of 20 km s^{-1} centred at $v_{\mathrm{LSR}} = 106.2$ km s^{-1}, excluding RFI-affected channels. No statistically significant features are seen over the entire $3° \times 3°$ field (3.5 x 3.5 kpc at a distance of 60 kpc). We have calculated the integrated line flux both at the central pixel and in a number of circular apertures with radii ranging from the half light radius of 13′ to 90′. Sample averaged spectra are shown in Figure 4, while corresponding mean column densities, $\langle N_{\mathrm{H\,I}} \rangle$, and H I masses, $M_{\mathrm{H\,I}}$, are given in Table 1. The quoted 1σ uncertainty has been calculated empirically by performing an identical analysis at 200 randomly-chosen central velocities located far from local Galactic emission and taking the dispersion of these measurements; this method implicitly takes into account systematics such as residual baseline-fitting errors in addition to the random error component.

Taking a 3σ upper limit, we conclude that there is no more than 100 M$_\odot$ of H I at velocities $96 \leq v_{\mathrm{LSR}} \leq$

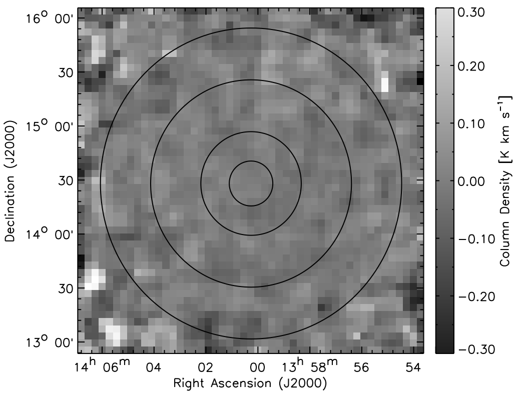

Figure 3. Zeroth moment map at the velocity of Boötes. Apertures of radius 13′ (the optical half-light radius), 30′, 60′, and 90′ are overplotted. The noise increases at the edges of the image due to the decreased integration time (see Figure 2).

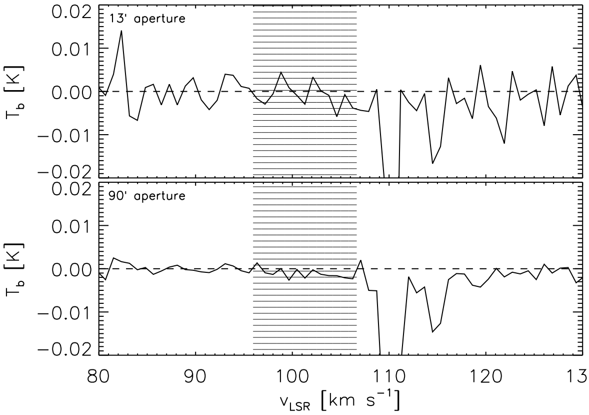

Figure 4. Spectra averaged over a 13′ *(top)* and 90′ *(bottom)* radius aperture centred on Boötes. The velocity range of the zeroth moment map (Figure 3) is represented by the shaded region.

107 km s^{-1} within the optical half-light radius of Boötes. Although we cannot measure an upper limit in the region of the spectrum affected by RFI, we can rule out any significant reservoir of H I, which would be evident in the clean part of the spectrum. If we assume that any emission at RFI-affected velocities is of similar magnitude to that in the clean part of the spectrum then the upper limit on the total H I mass within the optical half-light radius is 180 M$_\odot$. This assumption is likely to be valid unless the H I emission is much narrower than the emission seen in other dSphs (Blitz & Robishaw 2000) and offset to positive velocity with respect to the stars, a possibility we consider unlikely as gas removed by ram pressure stripping would trail the stars and appear offset to negative velocity. In an aperture with radius 90′ (1.6 kpc at a distance of 60 kpc) we find a 3σ upper limit of 4300 M$_\odot$ of H I at $96 \leq v_{\rm LSR} \leq 107$ km s^{-1}, and a total RFI-corrected H I mass upper limit of 8000 M$_\odot$. The 3σ column density limit within the beam is 1.5×10^{17} cm^{-2} at $96 \leq v_{\rm LSR} \leq 107$ km s^{-1} and 2.8×10^{17} cm^{-2} correcting for RFI-affected channels.

4 RESULTS FOR SGR LEADING TAIL

Putman et al. (2004) found no detections of positive velocity H I along the orbit of the Sagittarius dSph in the H I Parkes All-Sky Survey (HIPASS). The HIPASS observations north of the celestial equator reach an rms sensitivity of 11 mK with a spectral resolution of 26.4 km s^{-1}, corresponding to a column density 3σ upper limit of 1.6×10^{18} cm^{-2}.

In Figure 5 we present our zeroth moment map integrated over a velocity width of 20 km s^{-1} centred at $v_{\rm LSR} = 60$ km s^{-1}. These much deeper observations still reveal no evidence for any emission at the velocity of the Sagittarius leading tidal tail. Due to the polar orbit of Sagittarius, stream gas is expected to lie nearly parallel to lines of constant Galactic longitude, where $l = 0°$ is indicated by the dashed line in Figure 5. No features are found elongated in this direction. The column density 3σ upper limit averaged over the central 2×2 pixels is 2×10^{17} cm^{-2}. In an attempt to enhance any faint signal, we have calculated the mean column density in strips of constant l with widths, Δl, ranging from 15′ to 90′. An example for strips of width $\Delta l = 15'$, corresponding closely to the beam FWHM, is shown in Figure 6 and does not reveal any emission. We conclude that there is no H I associated with the leading Sagittarius tidal tail at this location down to a 3σ column density limit of 2×10^{17} cm^{-2}.

The leading tail also appears to be devoid of ionised gas, based on the non-detection of Hα emission at this location and velocity in the Wisconsin H-Alpha Mapper Northern Sky Survey (WHAM-NSS; Haffner et al. 2003) to a 3σ intensity upper limit of $I_{\rm H\alpha} < 0.025$ R. If ionised leading stream gas exists with the same column density as the neutral gas that is in the trailing tail, then its volume density must be less than $\bar{n}_{\rm H} < 0.002$ cm^{-3}, implying an unreasonably large line-of-sight depth of $L > 17$ kpc. However, a moderate reduction in the mean column density within the 1° WHAM beam could lower L to plausible values.

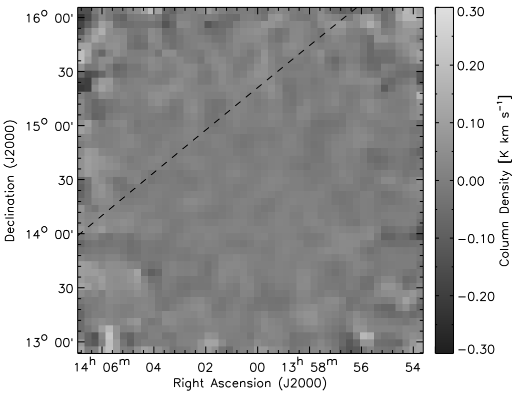

Figure 5. Zeroth moment map at the velocity of the Sagittarius leading tidal tail. The dashed line indicates $l = 0°$. Features associated with Sagittarius are expected to lie parallel to this line. The noise increases at the edges of the image due to the decreased integration time (see Figure 2).

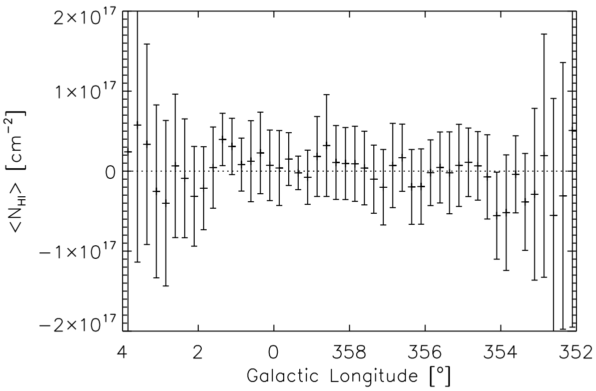

Figure 6. Mean H I column density in strips of constant Galactic longitude at the velocity range of Sagittarius debris. Strips are $\Delta l = 15'$ wide and include the region shown in Figure 5.

5 CONCLUSIONS

We detect no H I gas associated with the Boötes dSph galaxy down to a 3σ column density limit of 2.8×10^{17} cm^{-2}, corresponding to a mass limit of 180 M$_\odot$ within the optical half-light radius and 8000 M$_\odot$ within 1.6 kpc of the optical galaxy. While the stellar body of Boötes appears distorted (Belokurov et al. 2006a), casting doubt on its morphological classification, the dearth of gas in Boötes clearly indicates that it is an early-type dSph galaxy.

In Figure 7 we plot the gas fraction of Boötes, as estimated by the ratio of the H I gas mass to the V-band luminosity, along with the other dSph companions to the Milky Way catalogued by Blitz & Robishaw (2000) (for Sagittarius we use the deeper limit of Burton & Lockman 1999). Our observations are more than 5 times deeper than those of the LDS; combined with the relative proximity of Boötes, we are able to detect much smaller quantities of H I than Blitz & Robishaw (2000). Boötes has the most stringent upper limit on its absolute H I mass of any Local Group galaxy, and is among the most gas-poor galaxies even relative to its extremely low luminosity, with a 3σ upper limit of $M_{\rm H\,I}/L_V < 0.002$ M$_\odot$/L$_\odot$. Only the much more lumi-

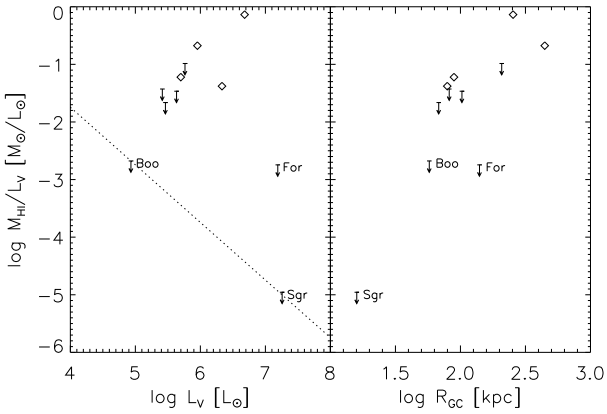

Figure 7. Gas fraction (ratio between H I gas mass and V-band luminosity) of dSph satellite galaxies of the Milky Way as a function of their V-band luminosity, L_V, *(left)*, and galactocentric radius, R_{GC}, *(right)*. The upper limit on the total H I mass of Boötes within the optical half-light radius is 180 $M_\odot$ (§ 3) and the upper limit for Sagittarius is 200 $M_\odot$ (Burton & Lockman 1999). All other H I masses and upper limits are from Blitz & Robishaw (2000). A dotted line of constant H I mass is shown in the left panel. Exceptionally gas-poor galaxies are labelled.

nous Sagittarius and Fornax dSphs are known to be more gas-poor.

Boötes has converted only a small fraction of its primordial baryons into stars. The leftover gas is no longer part of Boötes as would be expected if self-regulated star formation had been the only process operating. Unless reionisation prevented cool gas from falling onto Boötes at early times, gas must have been removed by tidal forces, ram pressure stripping, or supernova feedback. The proximity-gas mass relation (Blitz & Robishaw 2000; Figure 7) argues strongly against supernova feedback as the primary mechanism, since it occurs in all environments. Neither streams of stripped gas nor outflowing gas from Boötes are detected, indicating that these gas removal processes have either already completed or have left streams too tenuous to be detected with current observations. As Boötes lies on the fundamental line (Prada & Burkert 2002), the explanation for such a mass-metallicity relation cannot be entirely due to inefficient self-regulated star formation but must be partially driven, or at least not disrupted, by the extreme gas loss or primordial deficit in cool gas experienced by this low luminosity galaxy.

We detect no neutral gas associated with the leading Sagittarius tidal tail down to a 3σ column density limit of 2×10^{17} cm^{-2}. If the gas detected along the trailing tail (Putman et al. 2004) had been tidally stripped along with the stars, then a leading tail of gas would also exist. Either this leading tail is ionised, which would require it to have a lower density than the trailing tail, or the gas in the trailing tail was removed by ram pressure stripping before the tidal disruption of the parent galaxy began.

No other non-Galactic emission is detected at $-400 \leq v_{\rm LSR} \leq 450$ km s^{-1} over the entire 6°× 8° field.

ACKNOWLEDGMENTS

The Parkes Observatory is operated by the Australia Telescope National Facility, a division of the Commonwealth Scientific and Industrial Research Organisation. The Wisconsin H-Alpha Mapper is funded by the National Science Foundation. We thank John Reynolds, Andrew Hunt, and Jay Lockman for useful discussions. JB thanks the Australian Research Council for financial support.

REFERENCES

Belokurov, V. et al. 2006a, ApJ, 647, L111
Belokurov, V. et al. 2006b, ApJ, in press, astro-ph/0608448
Blitz, L., & Robishaw, T. 2000, ApJ, 541, 675
Brooks, A. M., Governato, F., Booth, C. M., Willman, B., Gardner, J. P., Wadsley, J., Stinson, G., Quinn, T. 2006, ApJL, submitted, astro-ph/0609620
Bullock, J. S., Kravtsov, A. V., Weinberg, D. H. 2000, ApJ, 539, 517
Burton, W. B., Lockman, F. J. 1999, A&A, 349, 7
Connors, T. W., Kawata, D., Gibson, B. K. 2006, MNRAS, 371, 108
Dekel, A., Woo, J. 2003, MNRAS, 344, 1131
Dong, S., Lin, D. N. C., Murray, S. D. 2003, ApJ, 596, 930
Grebel, E. K., Gallagher, III, J. S., Harbeck, D. 2003, AJ, 125, 1926
Grillmair, C. J. 2006, ApJ, 645, L37
Haffner, L. M., Reynolds, R. J., Tufte, S. L., Madsen, G. J., Jaehnig, K. P., Percival, J. W. 2003, ApJS, 149, 405
Hartmann, D., Burton, W. B. 1997, Atlas of Galactic Neutral Hydrogen (Cambridge University Press)
Kalberla, P. M. W., Burton, W. B., Hartmann, D., Arnal, E. M., Bajaja, E., Morras, R., Pöppel, W. G. L. 2005, A&A, 440, 775
Kennicutt, Jr., R. C. 1998, ApJ, 498, 541
Kepner, J. V., Babul, A., Spergel, D. N. 1997, ApJ, 487, 61
Klypin, A., Kravtsov, A. V., Valenzuela, O., Prada, F. 1999, ApJ, 522, 82
Mateo, M. L. 1998, ARA&A, 36, 435
Mayer, L., Mastropietro, C., Wadsley, J., Stadel, J., Moore, B. 2006, MNRAS, 369, 1021
Moore, B., Ghigna, S., Governato, F., Lake, G., Quinn, T., Stadel, J., Tozzi, P. 1999, ApJ, 524, L19
Muñoz, R. R., Carlin, J. L., Frinchaboy, P. M., Nidever, D. L., Majewski, S. R., Patterson, R. J. 2006, ApJ, 650, L51
Prada, F., Burkert, A. 2002, ApJ, 564, L73
Putman, M. E., Thom, C., Gibson, B. K., Staveley-Smith, L. 2004, ApJ, 603, L77
Read, J. I., Pontzen, A. P., Viel, M. 2006, MNRAS, 371, 885
Siegel, M. H. 2006, ApJ, 649, L83
Staveley-Smith, L. et al. 1996, PASA, 13, 243
Tassis, K., Kravtsov, A. V., Gnedin, N. Y. 2006, ApJ, submitted, astro-ph/0609763
Williams, D. R. W. 1973, A&AS, 8, 505
Willman, B. et al. 2005, ApJ, 626, L85
Zucker, D. B. et al. 2006a, ApJ, 643, L103
Zucker, D. B. et al. 2006b, ApJ, 650, L41